Volume 6, Issue 5, 2016, 1573 - 1579 ISSN 2069-5837

Biointerface Research in Applied Chemistry

www.BiointerfaceResearch.com

Original Research Article Open Access Journal

Received: 20.08.2016 / Revised: 25.09.2016 / Accepted: 10.10.2016 / Published on-line: 13.10.2016

Influence of position-dependent effective mass, position-dependent dielectric screening function and anisotropy on the binding energy and interband emission energy of impurity doped Quantum dots in presence of Gaussian white noise

Anuja Ghosh [1], Aindrila Bera [1], Manas Ghosh [1]

[1]*Department of Chemistry, Physical Chemistry Section, Visva Bharati University, Santiniketan, Birbhum 731 235, West Bengal, India.*

*corresponding author e-mail address: ***pcmg77@rediffmail.com***

ABSTRACT

The binding energy (BE) and interband emission energy (IEE) of impurity doped quantum dot (QD) have been examined in absence and presence of noise. Special emphasis has been put on effective mass and dielectric constant of the system as they become dependent on dopant location. Noise employed is a Gaussian white noise and it is added to the system in two different pathways viz. additive and multiplicative. Anisotropy, dopant location-dependent effective mass and dielectric constant alter the magnitude of BE and IEE from their values in case of constant effective mass and dielectric constant. Application of noise maintains the qualitative features of BE and IEE profiles that have been observed in absence of noise. However, presence of noise affects their magnitude in a way that perspicuously depends on their pathway of application. The findings reveal elegant routes of controlling the BE and IEE of doped QD system in presence of noise; especially when the effective mass and dielectric constant of system heavily depend on dopant co-ordinates.

Keywords: *quantum dot; impurity; anisotropy; position-dependent effective mass, position-dependent dielectric screening function; Gaussian white noise.*

1. INTRODUCTION

Low-dimensional semiconductor systems (LDSS) such as quantum wells (QWLs), quantum wires (QWRs) and quantum dots (QDs) are characterized by stringent quantum confinement which is much stronger in comparison with the bulk materials. In consequence, LDSS possess small energy separations between the subband levels and large value of electric dipole matrix elements. Introduction of impurity (dopant) into LDSS severely modifies their energy level distribution and naturally the *binding energy (BE)* is also noticeably changed. Thus, regulated incorporation of dopant can help manipulate the BE which possesses immense technological importance so far as nonlinear optical (NLO) properties of LDSS are concerned. As a result, we envisage rigorous research activities on LDSS doped with impurity [1–25].

Position-dependent effective mass (PDEM) of LDSS is an important topic that has drawn considerable attention in recent times. This is because of the fact that such a spatially varying mass leads to considerable change in the BE of the doped system (with respect to fixed effective mass) and thus visibly alters the NLO properties. In this context the works of Rajashabala and Navaneethakrishnan [26–28], Peter and Navaneethakrishnan [29], Khordad [30, 31], Qi et al. [32], Peter [33], Li et al. [34], and Naimi et al. [35] assume sufficient significance.

Dielectric screening function (DSF, ε) is of utmost importance as it can markedly change the BE and hence the NLO properties of LDSS. DSF can thus engineer the manufacturing of devices at desired frequencies by controlling the transitions associated with different electronic subbands [29]. Moreover, BE is also affected by *position-dependent DSF (PDDSF)*, $\varepsilon(r_0)$, leading to remarkable change in the optical and magnetic properties of doped LDSS [26]. PDDSF assumes further importance in view of describing screened interactions in real space [36]. Hence, of late, there are several studies on PDDSF by Peter and Navaneethakrishnan [29], Rajashabala and Navaneethakrishnan [26], Latha et al. [36], Köksal et al. [37], Jayam and Navaneethakrishnan [38] and Deng et al. [39].

Geometrical anisotropy is an important aspect that can hugely affect the BE and hence the NLO properties of LDSS. In reality, LDSS are mostly not at all isotropic which further vindicates the need of understanding how anisotropy affects BE and related optical properties. Experimentally, anisotropic QDs can be realized by chemically controlling the nanostructure aspect ratio [40]. Such anisotropic LDSS have generated unquestionable importance in view of fabrication of novel and useful technological devices. As a result, we find a lot of notable works on anisotropy in LDSS by Xie and his coworkers [40–43], Safarpour et. al. [44, 45] and Niculescu et al. [46], to mention a few.

Of late, we have made detailed investigations on how *noise* affects various NLO properties of impurity doped *GaAs* QDs with special emphasis on PDEM, PDDSF and anisotropy [47–49]. Recently, we have also worked on how interplay between hydrostatic pressure, temperature and noise can modulate the *interband emission energy (IEE)* of doped QD [50]. In the present study we meticulously investigate the profiles of BE and IEE of doped QD in presence of *Gaussian white noise* and under the purview of PDEM, PDDSF and anisotropy, without considering the effects of hydrostatic pressure and temperature. Such an investigation helps us understand more clearly the exclusive role

played by noise in shaping BE and IEE. The system under investigation is a 2-d QD (*GaAs*) containing single carrier electron and subject to parabolic confinement in the $x - y$ plane. The dopant impurity is modeled by a Gaussian potential in the presence of a perpendicular magnetic field which acts as an additional confinement. An external static electric field has been applied to the system. Gaussian white noise has been applied to the doped QD via two different pathways i.e. additive and multiplicative [47–50]. The findings reveal rich interplay between PDEM, PDDSF, anisotropy and noise (including its mode of application) that ultimately designs the BE and IEE profiles.

2. METHOD

The impurity doped QD Hamiltonian, in presence of external static electric field (F) applied along x and y-directions and spatially δ-correlated Gaussian white noise (additive/multiplicative) can be written as

$$H_0 = H_0' + V_{imp} + |e|F(x+y) + V_{noise}. \quad (1)$$

Under effective mass approximation, H_0' represents the 2-d quantum dot without impurity having single carrier electron under lateral parabolic confinement in the $x - y$ plane and in presence of a perpendicular magnetic field. $V(x,y) = \frac{1}{2}m^*\omega_0^2(x^2+y^2)$ is the confinement potential with ω_0 as the harmonic confinement frequency. H_0' is therefore given by

$$H_0' = \frac{1}{2m^*}\left[-i\hbar\nabla + \frac{e}{c}A\right]^2 + \frac{1}{2}m^*\omega_0^2(x^2+y^2). \quad (2)$$

m^*represents the effective mass of the electron inside the QD material. Using Landau gauge [A= (By, 0, 0), where A is the vector potential and B is the magnetic field strength], H_0' reads

$$H_0' = -\frac{\hbar^2}{2m^*}\left(\frac{\partial^2}{\partial x^2}+\frac{\partial^2}{\partial y^2}\right)+\frac{1}{2}m^*\omega_0^2x^2+\frac{1}{2}m^*\left(\omega_0^2+\omega_c^2\right)y^2 - i\hbar\omega_c y\frac{\partial}{\partial x} \quad (3)$$

$\omega_c = \frac{eB}{m^*c}$ being the cyclotron frequency, where c is the velocity of light. $\Omega = \sqrt{\omega_0^2+\omega_c^2}$ can be regarded as the effective confinement frequency in the y-direction. Pursuing the important works of Xie the ratio $\eta = \frac{\Omega}{\omega_0}$ could be defined as the *anisotropy parameter* [40, 41].

V_{imp} is the Gaussian impurity (dopant) potential [47–50] given by $V_{imp} = V_0 e^{-\gamma\left[(x-x_0)^2+(y-y_0)^2\right]}$. (x_0, y_0), V_0 and $\gamma^{-\frac{1}{2}}$ are the site of dopant incorporation, strength of the dopant potential, and the spatial spread of impurity potential, respectively. γ can be written as $\gamma = k\varepsilon$, where k is a constant and ε is the *static dielectric constant (SDC)* of the medium.

The dopant location-dependent effective mass i.e. PDEM; $m^*(r_0)$, is given by [26, 29]

$$\frac{1}{m^*(r_0)} = \frac{1}{m^*} + \left(1-\frac{1}{m^*}\right)\exp(-\beta r_0) \quad (4)$$

In the above expression $r_0 = \sqrt{x_0^2+y_0^2}$ is the dopant location and β is a constant having value 0.01 a.u. Above form of PDEM suggests that the dopant is strongly bound to the dot confinement center as $r_0 \to 0$ i.e. for on-center dopants whereas $m^*(r_0)$ becomes highly important as $r_0 \to \infty$ i.e. for far off-center dopants. The *Hermanson's* impurity position-dependent dielectric constant/dielectric screening function (PDDSF) is given by [26, 29, 36–39]

$$\frac{1}{\varepsilon(r_0)} = \frac{1}{\varepsilon} + \left(1-\frac{1}{\varepsilon}\right)\exp\left(-r_0/\alpha\right), \quad (5)$$

where ε is the SDC and α = 1.1 a.u. is the screening constant. The concept of SDC appears useful only for distances considerably away from the perturbation origin i.e. the impurity center. The choice of above form of PDDSF suggests that $\varepsilon(r_0) \to 1$ as $(r_0) \to 0$ i.e. for on-center dopants and approaches ε as $r_0 \to \infty$ i.e. for far off-center dopants. Such large r_0 can be viewed as the *screening radius* [36].

The term V_{noise} [cf. eqn.(1)] stands for white noise [$f(x, y)$] which follows a Gaussian distribution (generated by Box-Muller algorithm), has a strength ζ and is characterized by zero-average and spatial δ-correlation conditions [47–50]. Such white noise can be introduced to the system via two different modes (pathways) i.e. additive and multiplicative [47–50]. These two different modes can be discriminated on the basis of extent of system-noise interaction.

The time-independent Schrödinger equation has been solved by generating the sparse Hamiltonian matrix (H_0). The relevant matrix elements involve the function $\psi(x, y)$ which is a superposition of the products of harmonic oscillator eigenfunctions. In this context sufficient numbers of basic functions have been included after performing the convergence test. H_0 is diagonalized afterwards in the direct product basis of harmonic oscillator eigenfunctions to obtain the energy levels and wave functions. BE (E_B) for the ground state is defined as the difference between the ground state energies in absence and in presence of impurity and is given by

$$E_B = E_0 - E, \quad (6)$$

where E_0 is the ground state energy in absence of impurity and E is the same in presence of impurity. Following the works of Xia et al. [51, 52] and Revathi et al. [53] we can define IEE (E_{ph}) as

$$E_{ph} = E_0 + E_g - E_B, \quad (7)$$

where Eg is the band-gap energy of *GaAs* QD and is equal to ~ 1400 meV.

3. RESULTS AND DISCUSSION

The calculations are performed using the following parameters: the static dielectric constant (SDC): ε = 12.4, the fixed effective mass (FEM): $m^* = 0.067m_0$ (m_0 is the free electron mass), confinement potential: $\sim\omega_0$ = 250.0 meV, electric field strength: F = 100 KV/cm, magnetic field strength: B = 20.0 T, noise strength: ζ = 1.0 × 10−8, and dopant potential: V_0 = 280.0 meV. The parameters are suitable for *GaAs* QDs.

3.1. Role of anisotropy (η).

Figure 1a shows the pattern of variations of BE with anisotropy parameter η in absence of noise, in presence of additive noise and in presence of multiplicative noise, respectively. Under all conditions BE has been found to decrease with increase in anisotropy of the system. Similar profile has also been observed by Yang and Xie in absence of noise [43]. The profile indicates that an increase in the extent of anisotropy reduces the effective confinement of the system leading to fall in the binding energy. It has also been found that at a particular value of η the BE is lowest in presence of additive noise and highest in presence of multiplicative noise. BE under noise-free condition lies in between them.

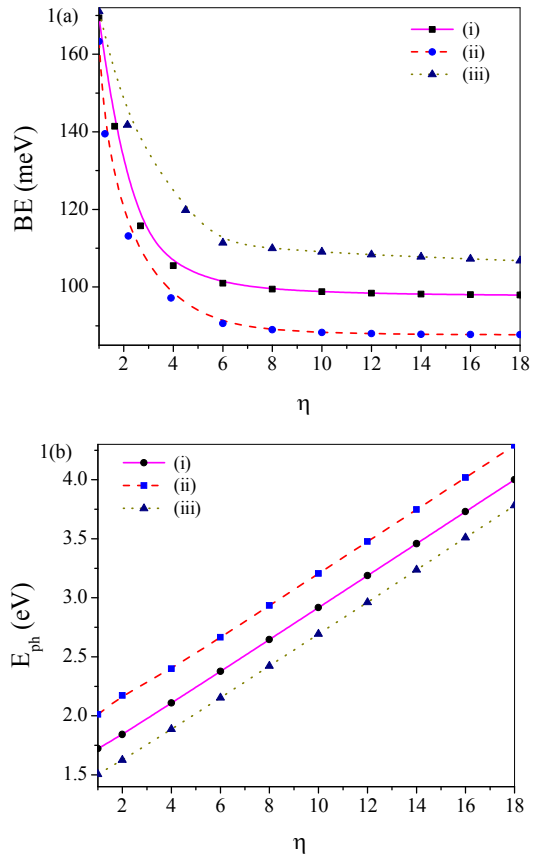

Figure 1. Plots of (a) BE vs η and (b) IEE vs η: (i) in absence of noise, (ii) in presence of additive noise and (iii) in presence of multiplicative noise.

Figure 1b displays the similar plot for IEE. In all the plots IEE has been found to increase with increase in η. The expression of IEE [cf. eqn (7)] suggests that it is the difference between E_0 and E_B which ultimately guides the IEE profile. An increase in anisotropy diminishes the BE of the system, which, in turn, enhances the $E_0 - E_B$ separation leading to enhancement of IEE. Thus, the qualitative features of variation of IEE with η remain unchanged even in presence of noise regardless of its mode of application. The plot also reveals that at a particular η the IEE is lowest in presence of multiplicative noise and highest in presence of additive noise. IEE under noise-free condition lies in between them.

3.2. Role of position-dependent effective mass $\left[m^*(r_0)\right]$.

Figure 2a exhibits the BE profiles against dopant location r_0 for *fixed effective mass (FEM)* $\left(m^* = 0.067m_0\right)$ and PDEM $\left[m^*(r_0)\right]$ in absence of noise and in presence of additive and multiplicative noise. The plots corresponding to FEM and PDEM are represented by dashed and solid lines, respectively. The profiles reveal a steady fall in the BE with increase in r_0

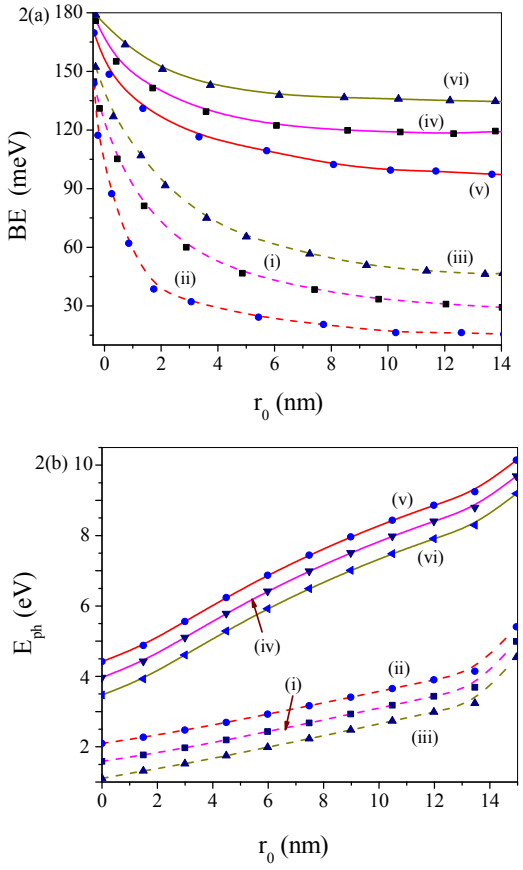

Figure 2. (a) Plot of BE vs r_0 : (i) using FEM under noise-free condition, (ii) using FEM in presence of additive noise, (iii) using FEM in presence of multiplicative noise, (iv) using PDEM under noise free condition, (v) using PDEM in presence of additive noise and (vi) using PDEM in presence of multiplicative noise; (b) Plot of IEE vs r_0 : (i) using FEM under noise-free condition, (ii) using FEM in presence of additive noise, (iii) using FEM in presence of multiplicative noise, (iv) using PDEM under noise-free condition, (v) using PDEM in presence of additive noise and (vi) using PDEM in presence of multiplicative noise.

I.e. with gradual shift of dopant from on-center to more and more off-center locations. Moreover, BE values with PDEM have been found to be greater than that with FEM. The findings of Peter and Navaneethakrishnan [29], Peter [33], Khordad [30] and Li et al. [34] also run in conformity with our observations in absence of noise. The observations suggest that such progressive shift of dopant from on-center to off-center locations diminishes the effective confinement of the system forcing BE to fall. Moreover, using PDEM, the fall in the effective confinement of the system with increase in r_0 appears to be much less intense than with FEM. In consequence, we observe greater BE values in case of PDEM in comparison with FEM. Application of noise does not qualitatively change the pattern of BE profile. However, the magnitude of BE values in absence and presence of noise (including its mode of application) follows the same sequence as found in case of anisotropy.

Fig. 2b depicts the similar plot for IEE. In all the plots IEE has been found to increase with increase in r_0. As before, the enhancement of $E_0 - E_B$ separation with r_0 (due to drop in BE with shift of dopant from on-center to off-center locations) appears to be responsible for such an increase. Thus, the qualitative features of variation of IEE with r_0 remain unchanged also in presence of noise independent of its mode of application. The plots further reveal higher magnitude of IEE using PDEM than using FEM suggesting greater $E_0 - E_B$ separation in case of the former. The magnitude of IEE in absence and presence of noise (including its mode of application) maintains the same sequence as found in case of anisotropy.

3.3. Role of position-dependent dielectric screening function $\left[\varepsilon(r_0)\right]$.

Figure 3a delineates the BE profiles against dopant location r_0 for *static dielectric constant (SDC)* (ε = 12.4) and PDDSF $\left[\varepsilon(r_0)\right]$ in absence of noise and in presence of additive and multiplicative noise. The plots corresponding to SDC and PDDSF are represented by dashed and solid lines, respectively. The profiles reveal a steady decline in the BE with increase in r_0 i.e. with progressive shift of dopant from on-center to more and more off-center locations. Furthermore, BE values with PDDSF have been found to be larger than that with SDC. We have come across similar observations in the works of Peter and Navaneethakrishnan [29] and Deng et al. [39] in absence of noise. The observations, therefore, indicate that such persistent shift of dopant from on-center to off-center locations depletes the effective confinement of the system leading to fall of BE. Moreover, using PDDSF, the fall in the effective confinement of the system with increase in r_0 appears to be much more pronounced than with SDC. In consequence, we observe greater fall in BE values in case of PDDSF in comparison with SDC.

Application of noise does not cause any characteristic change of the overall pattern of BE profile. However, the magnitude of BE values in absence and presence of noise (including its mode of application) follows the same sequence as found earlier.

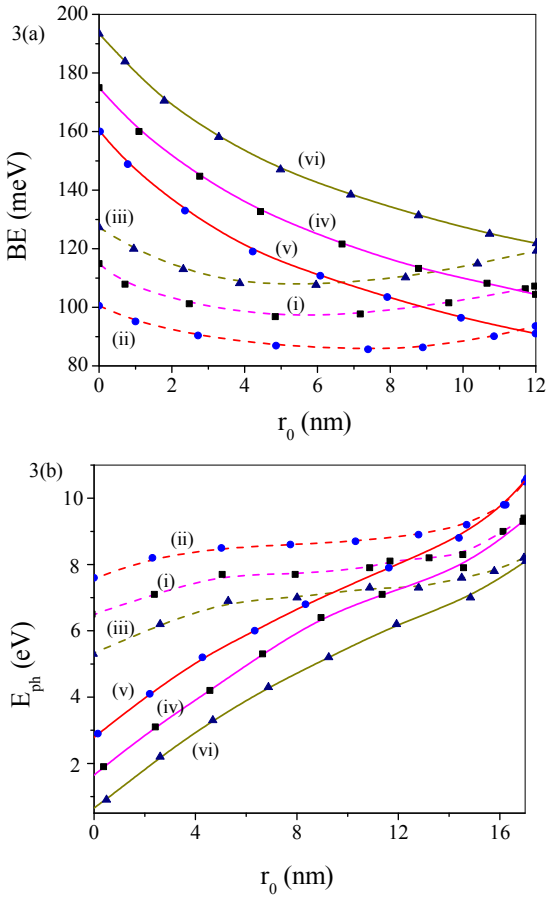

Figure 3. (a) Plot of BE vs r_0 : (i) using SDC under noise-free condition, (ii) using SDC in presence of additive noise, (iii) using SDC in presence of multiplicative noise, (iv) using PDDSF under noise free condition, (v) using PDDSF in presence of additive noise and (vi) using PDDSF in presence of multiplicative noise; (b) Plot of IEE vs r_0 : (i) using SDC under noise-free condition, (ii) using SDC in presence of additive noise, (iii) using SDC in presence of multiplicative noise, (iv) using PDDSF under noise-free condition, (v) using PDDSF in presence of additive noise and (vi) using PDDSF in presence of multiplicative noise.

Figure 3b depicts the similar plot for IEE. In all the plots IEE has been found to increase steadily with increase in r_0. Here also, the enhancement of $E_0 - E_B$ gap with r_0 (due to drop in BE with shift of dopant from on-center to off-center locations) appears to be the key reason behind such an increase. However, the increase of IEE with r_0 appears much more pronounced using PDDSF than with SDC. Thus, the qualitative features of variation of IEE with r_0 remain unaltered even in presence of noise independent of its mode of application. The plots further divulge higher magnitude of IEE using PDDSF than using SDC suggesting greater $E_0 - E_B$ interval in case of the former. The magnitude of IEE in absence and presence of noise (including its mode of application) retains the same sequence as found erstwhile.

3.4. Role of noise strength (ζ).

At this point of discussion it needs to be noted that in all the plots BE values maintain a definite sequence viz. BE (in presence of multiplicative noise) >BE (in absence of noise) >BE (in presence of additive noise). It can therefore be inferred that, for a fixed extent of disorder introduced into the system, multiplicative noise enhances the effective confinement of the system over that of noise-free condition whereas additive noise does just the reverse. Driven by aforesaid outcome, we concentrate on the important aspect of how BE changes as noise strength (ζ) is varied over a range. Fig. 4a delineates the variation of BE with $-\log(\zeta)$ in presence of additive [Figure 4a (i)] and multiplicative [Figure 4a (ii)] noise, respectively. We have varied noise strength over a range from $\zeta = 1.0\times10^{-12}$ to $\zeta = 1.0\times10^{-2}$ and the BE values at the lowest end of the range nearly correspond to those under noise-free condition.

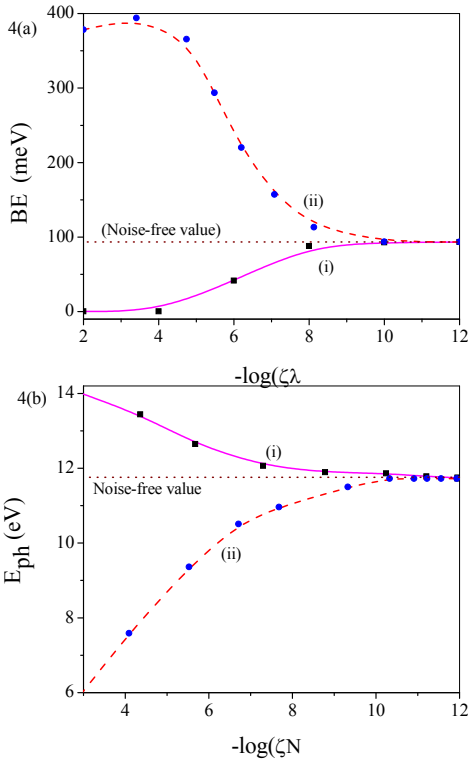

Figure 4. Plots of (a) BE vs $-\log(\zeta)$ and (b) IEE vs $-\log(\zeta)$:(i) in presence of additive noise and (ii) in presence of multiplicative noise.

It has been found that in case of additive noise BE decreases persistently with increase in ζ. On the other hand, BE follows exactly the reverse trend with increase in ζ for multiplicative noise. It thus appears that gradual enhancement in the extent of noise applied to the system may deplete or amplify the effective confinement depending on the mode of application of noise and results into steadfast drop/rise in BE. The enhancement of effective confinement of the system using multiplicative noise could have its origin in the close linkage of this particular mode with the system coordinates. Additive noise, on the other hand, makes a rather weak contact with the system that results into drop in the effective confinement and consequently in the BE.

In case of IEE we find a different sequence viz. IEE (in presence of additive noise) >IEE (in absence of noise) >IEE (in presence of multiplicative noise). It can therefore be inferred that, for a given size of disorder fed into the system, additive noise enhances IEE of the system over that of noise-free condition whereas multiplicative noise does just the reverse. Figure 4b depicts the similar plot for IEE. It has been found that in case of additive noise IEE increases monotonically with increase in ζ and follows exactly the opposite trend for multiplicative noise. It thus appears that gradual enhancement in the extent of noise applied to the system may deplete or amplify the difference ΔE (i.e. $E_0 - E_B$) depending evidently on the mode of application of noise leading to persistent drop/rise in IEE. The said mode actually controls the extent of interaction between noise and the system coordinates. Since additive and multiplicative noise interact with the system coordinates to varied extents, the difference ΔE behaves in diverse ways as noise strength enhances. Enhancement in noise strength augments ΔE when applied in an additive mode and reduces the same in case of multiplicative mode. The observed IEE profile simply follows the change in ΔE associated with the mode of application of noise.

4. CONCLUSIONS

The BE and IEE of impurity doped QD have been investigated in the light of interplay between anisotropy, PDEM, PDDSF, and noise. It has been found that BE decreases with increase in anisotropy of the system and with progressive shift of dopant from on-center to more off-center locations. Above observations come out to be true with FEM, PDEM, SDC and PDDSF, both in presence and absence of noise. IEE exhibits exactly the reverse behavior to BE. However, both BE and IEE display greater value using PDEM and PDDSF than using FEM and SDC, respectively. Application of noise does not bring about any qualitative alteration in the pattern of BE and IEE profiles from that of noise-free condition. However, noise monitors the magnitude of BE and IEE that depends conspicuously on mode of application of noise. BE reveals lowest value in presence of additive noise and highest in presence of multiplicative noise. BE under noise-free condition lies in between them. On the other

hand, IEE becomes lowest in presence of multiplicative noise and highest in presence of additive noise. IEE under noise-free condition lies in between them. With increase in noise strength BE decreases in case of additive noise and increases in case of multiplicative noise. IEE depicts exactly the opposite behavior to BE with variation of noise strength. The findings are expected to have technological relevance.

5. REFERENCES

[1] Tąs H., Şahin M., The electronic properties of core/shell/well/shell spherical quantum dot with and without a hydrogenic impurity, *Journal of Applied Physics*, 111, 8, 083702, **2012.**

[2] Tąs H., Şahin M., The inter-sublevel optical properties of a spherical quantum dot-quantum well with and without a donor impurity, *Journal of Applied Physics*, 112, 5, 053717, **2012.**

[3] Özmen A., Yakar Y., Çakír B., Atav Ü., Computation of the oscillator strength and absorption coefficients for the intersubband transitions of the spherical quantum dot, *Optics Communications*, 282, 19, 3999-4004, **2009.**

[4] Çakír B., Yakar Y., Özmen A., Refractive index changes and absorption coefficients in a spherical quantum dot with parabolic potential, *Journal of Luminescence*, 132, 10, 2659-2664, **2012.**

[5] Çakír B., Yakar Y., Özmen A., Özgür Sezer M., Şahin M., Linear and nonlinear optical absorption coefficients and binding energy of a spherical quantum dot, *Superlattices and Microstructures*, 47, 4, 556-566, **2010.**

[6] Zeng Z., Garoufalis C.S., Terzis A.F., Baskoutas S., Linear and nonlinear optical properties of *ZnS/ZnO* core shell quantum dots: Effect of shell thickness, impurity, and dielectric environment, *Journal of Applied Physics*, 114, 2, 023510, **2013.**

[7] Baskoutas S., Paspalakis E., Terzis A.F., Electronic structure and nonlinear optical rectification in a quantum dot: effects of impurities and external electric field, *Journal of Physics: Condensed Matter*, 19, 39, 395024, **2007.**

[8] Karabulut İ., Baskoutas S., Linear and nonlinear optical absorption coefficients and refractive index changes in spherical quantum dots: Effects of impurities, electric field, size, and optical intensity, *Journal of Applied Physics*, 103, 7, 073512, **2008.**

[9] Karabulut İ., Atav Ü., Şafak H., Tomak M., Linear and nonlinear intersubband optical absorptions in an asymmetric rectangular quantum well, *European Physical Journal B*, 55, 3, 283-288, **2007.**

[10] Karabulut İ., Baskoutas S., Second and third harmonic generation susceptibilities of spherical quantum dots: Effects of impurities, electric field and size, *Journal of Computational and Theoretical Nanoscience*, 6, 1, 153-156, **2009.**

[11] Gülveren B., Atav Ü., Şahin M., Tomak M., A parabolic quantum dot with *N* electrons and an impurity, *Physica E*, 30, 1-2, 143-149, **2005.**

[12] Khordad R., Bahramiyan H., Impurity position effect on optical properties of various quantum dots, *Physica E*, 66, 107-115, **2015.**

[13] Kumar K.M., Peter A.J., Lee C.W., Optical properties of a hydrogenic impurity in a confined $Zn_{1-x}Cd_xSe/ZnSe$ quantum dot, *Superlattices and Microstructures*, 51, 1, 184-193, **2012.**

[14] Niculescu E.C., Dielectric mismatch effect on the photo-ionization cross section and intersublevel transitions in *GaAs* nanodots, *Optics Communications*, 284, 13, 3298-3303, **2011.**

[15] Duque C.A., Mora-Ramos M.E., Kasapoğlu E., Ungan F., Yesilgul U., Şakiroğlu S., Sari H., Sökmen I., Impurity-related linear and nonlinear optical response in quantum-well wires with triangular cross section, *Journal of Luminescence*, 143, 304-313, **2013.**

[16] Kasapoğlu E., Ungan F., Sari H., Sökmen I., Mora-Ramos M.E., Duque C.A., Donor impurity states and related optical responses in triangular quantum dots under applied electric field, *Superlattices and Microstructures*, 73, 171-184, **2014.**

[17] Tiutiunnyk A., Tulupenko V., Mora-Ramos M.E., Kasapoğlu E., Ungan F., Sari H., Sökmen I., Duque C.A., Electron-related optical responses in triangular quantum dots, *Physica E*, 60, 127-132, **2014.**

[18] Rezaei G., Vahdani M.R.K., Vaseghi B., Nonlinear optical properties of a hydrogenic impurityin an ellipsoidal finite potential quantum dot, *Current Applied Physics*, 11, 2, 176-181, **2011.**

[19] Vahdani M.R.K., Rezaei G., Linear and nonlinear optical properties of a hydrogenic donor in lens-shaped quantum dots, *Physics Letters A*, 373, 34, 3079-3084, **2009.**

[20] Rezaei G., Vaseghi B., Taghizadeh F., Vahdani M.R.K., Karimi M.J., Intersubband optical absorption coefficient changes and refractive index changes in a two-dimensional quantum pseudodot system, *Superlattices and Microstructures*, 48, 5, 450-457, **2010.**

[21] Barseghyan M.G., Kirakosyan A.A., Duque C.A., Donor-impurity related binding energy and photoionization cross-section in quantum dots: electric and magnetic fields and hydrostatic pressure effects, *European Physical Journal B*, 72, 4, 521-529, **2009.**

[22] Mughnetsyan V.N., Barseghyan M.G., Kirakosyan A.A., Binding energy and photoionization cross section of hydrogen-like donor impurity in quantum well-wire in electric and magnetic fields, *Superlattices and Microstructures*, 44, 1, 86-95, **2008.**

[23] Ribeiro F.J., Latgé A., Pacheco M., Barticevic Z., Quantum dots under electric and magnetic fields: Impurity-related electronic properties, *Journal of Applied Physics*, 82, 1, 270-274, **1997.**

[24] Duque C.A., Porras-Montenegro N., Pacheco M., Oliveira L.E., Effects of applied magnetic fields and hydrostatic pressure on the optical transitions in self-assembled *InAs/GaAs* quantum dots, *Journal of Physics: Condensed Matter*, 18, 6, 1877, **2006.**

[25] Duque C.A., Porras-Montenegro N., Barticevic Z., Pacheco M., Oliveira L.E., Electron-hole transitions in self-assembled *InAs/GaAs* quantum dots: Effects of applied magnetic fields and hydrostatic pressure, *Microelectronics Journal*, 36, 3, 231-233, **2005.**

[26] Rajashabala S., Navaneethakrishnan K., Effects of dielectric screening and position dependent effective mass on donor binding energies and on diamagnetic susceptibility in a quantum well, *Superlattices and Microstructures*, 43, 3, 247-261, **2008.**

[27] Rajashabala S., Navaneethakrishnan K., Effective masses for donor binding energies in quantum well systems, *Modern Physics Letters B*, 20, 24, 1529-1541, **2006.**

[28] Rajashabala S., Navaneethakrishnan K., Effective masses for donor binding energies in nonmagnetic and magnetic quantum well systems: effect of magnetic field, *Brazilizn Journal ofPhyics*, 37, 3, 1134-1140, **2007.**

[29] Peter A.J., Navaneethakrishnan K., Effects of position-dependent effective mass and dielectric function of a hydrogenic donor in a quantum dot, *Physica E*, 40, 8, 2747-2751, **2008.**

[30] Khordad R., Effects of position-dependent effective mass of a hydrogenic donor impurity in a ridge quantum wire, *Physica E*, 42, 5, 1503-1508, **2010.**

[31] Khordad R., Effect of position-dependent effective mass on linear and nonlinear optical properties of a cubic quantum dot, *Physica B*, 406, 20, 3911-3916, **2011.**

[32] Qi X.-H., Kang X.-J., Liu J.-J., Effect of a spatially dependent effective mass on the hydrogenic impurity binding energy in a finite parabolic quantum well, *Physical Review B*, 58, 16, 10578-10582, **1998.**

[33] Peter A.J., The effect of position-dependent effective mass of hydrogenic impurities in parabolic *GaAs/GaAlAs* quantum dots in a strong magnetic field, *International Journal of Modern Physics B*, 23, 26, 5109-5118, **2009.**

[34] Li Y.-X., Liu J.-J., Kang X.-J., The effect of a spatially dependent effective mass on hydrogenic impurity binding energy in a finite parabolic quantum well, *Journal of Applied Physics*, 88, 5, 2588-2592, **2000.**

[35] Naimi Y., Vahedi J., Soltani M.R., Effect of position-dependent effective mass on optical properties of spherical nanostructures, *Optical and Quantum Electronics*, 47, 8, 2947-2956, **2015.**

[36] Latha M., Rajashabala S., Navaneethakrishnan K., Effect of dielectric screening on the binding energies and diamagnetic

susceptibility of a donor in a quantum well wire, *Physica Status Solidi B*, 243, 6, 1219-1228, **2006.**

[37] Köksal M., Kilicarslan E., Sari H., Sökmen I., Magnetic-field effect on the diamagnetic susceptibility of hydrogenic impurities in quantum well-wires, *Physica B*, 404, 21, 3850-3854, **2009.**

[38] Jayam Sr. G., Navaneethakrishnan K., Effects of electric field and hydrostatic pressure on donor binding energies in a spherical quantum dot, *Solid State Communications*, 126, 12, 681-685, **2003.**

[39] Deng Z.-Y., Guo J.-K., Lai T.-R., Impurity states in a spherical $GaAs.Ga_{1-x}Al_xAs$ quantum dot: Effects of the spatial variation of dielectric screening, *Physical Review B*, 50, 8, 5736-5739, **1994.**

[40] Xie W., Optical anisotropy of a donor in ellipsoidal quantum dots, *Physica B*, 407, 23, 4588-4591, **2012.**

[41] Xie W., Third-order nonlinear optical susceptibility of a donor in elliptical quantum dots, *Superlattices and Microstructures*, 53, January, 49-54, **2013.**

[42] Chen T., Xie W., Nonlinear optical properties of a three-dimensional anisotropic quantum dot, *Solid State Communications*, 152, 4, 314-319, **2012.**

[43] Yang L., Xie W., Photoionization cross section of a donor impurity in a two-dimensional anisotropic quantum dot, *Physica B*, 407, 18, 3884-3887, **2012.**

[44] Safarpour Gh., Izadi M.A., Novzari M., Niknam E., Moradi M., Anisotropy effect on the nonlinear optical properties of a three-dimensional quantum dot confined at the center of a cylindrical nano-wire, *Physica E*, 59, 124-132, **2014.**

[45] Safarpour Gh., Izadi M.A., Novzari M., Yazdanpanahi S., Anisotropy effect on the linear and nonlinear optical properties of a laser dressed donor impurity in a *GaAs/GaAlAs* nanowire superlattice., *Superlattices and Microstructures*, 75, 936-947, **2014.**

[46] Niculescu E.C., Burileanu L.M., Radu A., Lupąscu A., Anisotropic optical absorption in quantum well wires induced by high-frequency laser fields, *Journal of Luminescence*, 131, 6, 1113-1120, **2011.**

[47] Sarkar S., Ghosh A.P., Mandal A., Ghosh M., Modulating nonlinear optical properties of impurity doped Quantum dots via the interplay between anisotropy and Gaussian white noise, *Superlattices and Microstructures*, 90, 297-307, **2016.**

[48] Ghosh A.P., Mandal A., Sarkar S., Ghosh M., Influence of position-dependent effective mass on the nonlinear optical properties of impurity doped Quantum dots in presence of Gaussian white noise, *Optics Communications*, 367, 15, 325-334, **2016.**

[49] Bera A., Ganguly J., Saha S., Ghosh M., Interplay between noise and position-dependent dielectric screening function in modulating nonlinear optical properties of impurity doped quantum dots, *Optik*, 127, 16, 6771-6778, **2016.**

[50] Bera A., Ghosh M., Combined influence of hydrostatic pressure and temperature on interband emission energy of impurity doped quantum dots in presence of noise, *Physica B*, 500, 24-31, **2016.**

[51] Xia C.-X., Jiang F., Wei S., Hydrostatic pressure effects on exciton states in *InAs/GaAs* quantum dots, *Superlattices and Microstructures*, 43, 4, 285-291, **2008.**

[52] Xia C.-X., Wei S., Quantum size effect on excitons in zinc-blende *GaN/AlN* quantum dot, *Microelectronics Journal*, 37, 11, 1408-1411, **2006.**

[53] Revathi M., Peter A.J., Donor bound excitons confined in a $GaN/Ga_{1-x}Al_xN$ quantum dot, *Solid State Communications*, 150, 17-18, 816-819, **2010.**

6. ACKNOWLEDGEMENTS

The authors A.G., A.B. and M.G. thank D.S.T-F.I.S.T (Govt. of India) and U.G.C.- S.A.P (Govt. of India) for support.